ELSEVIER

Chemical Engineering Journal 134 (2007) 200–208

Chemical Engineering Journal

www.elsevier.com/locate/cej

Modeling of industrial reactor for hydrotreating of vacuum gas oils Simultaneous hydrodesulfurization, hydrodenitrogenation and hydrodearomatization reactions

F. Jiménez [a], V. Kafarov [a,*], M. Nuñez [b]

[a] *Industrial University of Santander, Kra 27 Calle 9, Bucaramanga, Colombia*
[b] *Colombian Petroleum Institute-ICP, Piedecuesta, Colombia*

Abstract

The modeling of an industrial trickle bed reactor (TBR) for hydrotreating (HDT) of vacuum gas oils (VGO) and other heavy fractions oils was developed based on experiments carried out under typical industrial conditions at pilot plant. Simultaneous reactions for hydrodesulfurization (HDS), hydrodenitrogenation (HDN), hydrodearomatization (HDA) and inhibition effects among different molecules such as decahydro-naphtalene, naphthalene, anthracene (mono-, di-, tri-aromatic), carbazole (non-basic nitrogen), acridine (basic nitrogen), dibenzotiophene (sulfur), and water, mixed with a vacuum gas oil severely hydrotreated (matrix feed), were taken into account. Analytical techniques selected for this research were nuclear magnetic resonance (NMR), for aromatic content and other analysis, ultra violet–visible spectrometry (UV–vis), for aromatic families, simulated distillation (SimDis), and standard tests (ASTM) to determinate basic nitrogen, total nitrogen, total sulfur, and other physicochemical properties of vacuum gas oils.

Keywords: Industrial reactor; Modeling; Hydrotreating; HDS; HDN; HDA; Inhibition effects

1. Introduction

It is well known that hydrotreatment is used in the refining industry to remove contaminants such as sulfur (HDS), nitrogen (HDN), metals (HDM), etc., mainly because of technical and environmental reasons [1]. Better understanding of HDS has been acquired over the last decades through process development; however, most of the available information has been obtained from studies of light fractions, or synthetic solvents and model molecules [2]. Thus, mathematical models for heavier fractions, such as vacuum gas oil, and for simultaneous HDS, HDN and HDA are limited in literature, probably because of the need for specific data on these heavy fractions, and also due to the incomplete or less precise results about mutual inhibitions. For these reasons, the aim of this work was the modeling of an industrial reactor (including HDS, HDN and HDA reactions) based on experiments carried out under typical industrial conditions at pilot plant, and the selection of adequate analytical techniques for the investigation of transformations during the HDT, taking into account inhibition or promotion effects of sulfur, nitrogen, and aromatic compounds during HDT of vacuum gas oils. The strategy used for this research includes five steps: experimental part, analytical part, construction of kinetic expressions, evaluation of inhibition effects, and modeling of industrial reactor. These steps are summarized in Fig. 1.

2. Experimental

2.1. Materials

2.1.1. Feed oil

Gas oil from an intermediate crude oil (naphtenic/paraffinic, 27° API, 0.8% S) was selected as main feed oil for kinetic and inhibition analysis. The selected gas oil (VGO) was distillated into four fractions at pilot plant (lowest to heaviest: Ct-I, Ct-II, Ct-III and Ct-IV) and taken to the hydrotreating process (VGOH). Each fraction of VGO and VGOH was properly analyzed. The properties of the initial fractions and their hydrotreated products were studied at several temperatures: 330, 350 and 370 °C. The results for feed and hydrotreated fractions at 350 °C are shown in Table 1.

* Corresponding author. Tel.: +57 76344746; fax: +57 76344684.
E-mail address: kafarov@uis.edu.co (V. Kafarov).

1385-8947/$ – see front matter © 2007 Elsevier B.V. All rights reserved.
doi:10.1016/j.cej.2007.03.080

Nomenclature

a'_v	gas–liquid interfacial area per unit reactor volume
a''_v	liquid–solid interfacial area per unit reactor volume
C^s_{is}	molar concentration of fluid reactant i at surface of solid
C_i	molar concentration of component i
C_{iS}	molar concentration of i inside the solid
d_p	equivalent particle diameter
d_r	reactor diameter
D_{ei}	effective diffusivity of component i for transport
F_i	molar flow rate of component i
H_i	Henry's law coefficient, partial molar enthalpy of species i
k	reaction rate coefficient
k_G	mass transfer coefficient from gas to gas–liquid interface
k_L	mass transfer coefficient from gas–liquid interface to liquid bulk
k_l	liquid–solid mass transfer coefficient
K_i	adsorption equilibrium constant of component i
K_L	overall mass transfer coefficient in terms of liquid concentration gradient
n	reaction order
N	number of species
N_r	number of reactions
$N_{GL,i}$ a_{GL}	mass transfer coefficient from gas to gas–liquid interface
$N_{LS,i}$ a_{LS}	liquid–solid mass transfer coefficient
P_t	total pressure
r_j	reaction rate of reaction j per unit catalyst mass for heterogeneous reaction
R	Gas law constant
S	stoichiometric coefficient matrix ($S_{j,i}$)
T	absolute temperature (K)
U_{sG}	superficial gas velocity
U_{sL}	superficial liquid velocity
z	axial coordinate in reactor

Greek symbols

ε	bed void fraction
μ_G	gas viscosity
μ_L	liquid viscosity
ρ_B	catalyst bulk density
ρ_f	fluid density
ρ_G	gas density
ρ_L	liquid density
ρ_s	density of the catalyst

Subscripts and superscripts

A	aromatics
DBT	dibenzothiophene
G	gas phase
H_2	molecular hydrogen
H_2S	hydrogen sulfide
i	component i
in	input
I	interface
L	liquid phase
N_{NB}	non-basic nitrogen
N_B	basic nitrogen
out	output
p	pellet
s	inside solid; also superficial velocity

2.1.2. Catalyst

A combination of different commercial Ni-Mo/Al_2O_3 catalysts, similar to the configuration used in the industrial reactor in the Refinery of Barrancabermeja, Ecopetrol (Colombian Petroleum Company), was employed. The catalysts shape is like a trilobe, they have an average equivalent size of 1.8 mm, a length of 4.1 mm, and are mixed (diluted) with spherical and inert SiC particles of different sizes, with the purpose of improving the flow pattern and help to achieve isothermal conditions.

2.1.3. Reactive

To detect inhibition or promotion effects during hydrotreating, and based on specific review and technical evaluation, six pure commercially available chemicals were purchased: decahydro-naphtalene (99%) and naphthalene (98%) were obtained from Aldrich, anthracene from Baker, carbazole (>96%), acridine (>97%) and dibenzotiophene (>98%) were obtained from Fluka. Emulsified water into the feed oil (5–10 vol.%) was also considered. The selected chemicals were mixed, at similar concentrations with the real feedstock, into a severely hydrotreated vacuum gas oil, under an elaborated factorial design of experiments (2^5) and then submitted to the hydrotreating process.

2.2. Equipment and procedures

2.2.1. Pilot plant

All the hydrotreating tests were carried out in a pilot plant, located in the Colombian Petroleum Institute (ICP—Ecopetrol). Basically, the pilot unit has four sections: (1) feed section, the liquid oil is preheated and mixed with pure hydrogen, in upflow operation; (2) reaction section, the trickle bed reactor has an inside diameter of 1.9 cm and a length of 73.5 cm, whereas the temperature is measured by four thermocouples and maintained constant by means of a thermowell; (3) products section, the reactor outlet is led to a high pressure and temperature separator where the liquid and the gas are separated; and (4) gases section, the gas exiting is passed through a caustic trap before being released; the schematic diagram of the pilot unit is shown in Fig. 2.

2.2.2. Operative conditions

The ranges of operating conditions for hydrotreating tests were: for temperature 330–390 °C, for pressure 6–10 MPa, for

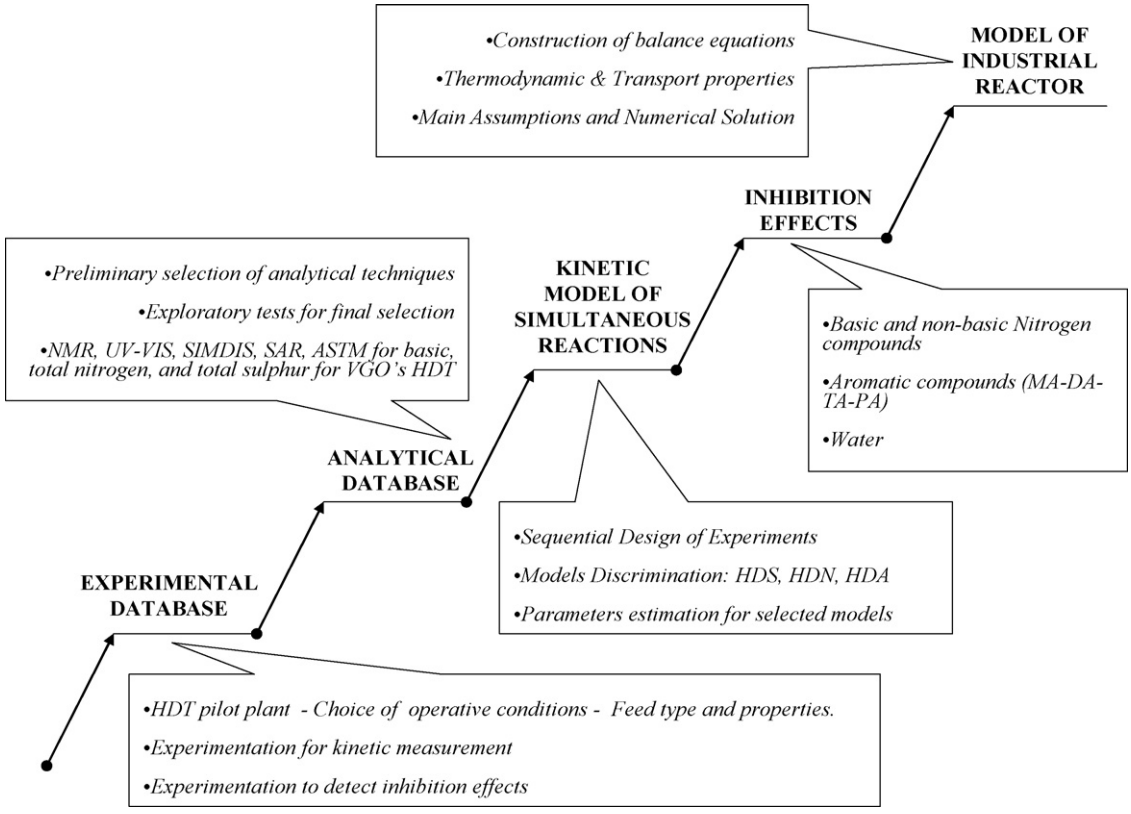

Fig. 1. General scheme of the strategy followed for the present research.

Table 1
Feed oil and hydrotreated product properties (VGO and VGOH)

	VGO	VGO Ct-I	VGO Ct-II	VGO Ct-III	VGO Ct-IV	VGOH Ct-I	VGOH Ct-II	VGOH Ct-III	VGOHCt-IV
Fraction (wt%)	100	14.5	59.1	10.8	15.6				
Range of boiling points (°C)		IBP-371	371–482	482–510	510-FBP	223-399	318−490	423−527	463−642
Standard tests									
Density at 15 °C (g/mL)	0.9185	0.889	0.9153	0.9355	0.9573	0.8878	0.9048	0.9189	0.9346
API (°)	22.5	27.6	23	19.7	16.2	27.8	24.8	22.6	19.8
Refraction index at 70 °C (N/A)	1.491	1.473	1.488	1.501	1.5181	1.4704	1.4809	1.490	1.5007
Sulfur (wt%)	0.805	0.56	0.75	0.94	1.24	0.12	0.18	0.21	0.26
Total nitrogen (ppm)	1546	467.1	1238	2240	3136	353.2	547.9	1198	2159
Basic nitrogen (ppm)	490	140	420	690	930	90	330	580	720
Aromatics (wt%)									
Mono-aromatic	4.56	5.11	4.56	4.28	4.15	9.53	5.95	5.26	4.76
Di-aromatic	3.73	5.4	3.58	3.09	2.99	1.95	2.08	2.03	1.98
Tri-aromatic	3.98	3.38	4.32	4.07	3.85	1.64	2.19	2.24	2.28
Poly-aromatic	2.98	0.78	2.31	3.47	6.53	0.22	1.34	1.98	4.24
Hydrogen type (H NMR) (wt%)									
Tetra	0.15	0.05	0.13	0.17	0.27	0.034	0.093	0.138	0.214
Tri–tetra	0.52	0.30	0.50	0.57	0.76	0.147	0.299	0.413	0.548
Di–tri–tetra	2.87	3.21	2.73	2.74	3.16	1.60	1.63	1.88	2.02
Mono	1.78	1.73	1.73	1.86	1.95	2.72	2.08	1.91	1.96
CH, CH_2 alpha	4.89	4.68	4.75	4.86	5.63	5.14	3.99	3.99	4.34
CH_3 alpha	1.91	2.49	1.80	1.75	1.90	3.78	2.28	1.92	1.82
Alpha olefinic	1.32	1.17	1.28	1.33	1.60	1.53	1.27	1.24	1.44
CH, CH_2, beta HyAr	3.67	3.32	3.62	3.64	4.14	4.00	3.42	3.43	3.34
CH, CH_2 beta y + (chains)	57.35	54.19	57.78	57.47	58.55	53.56	58.62	60.09	61.07
CH_3 gamma y +	25.54	28.78	25.67	25.61	22.02	27.32	26.32	25.01	23.24
Total aromatic hydrogen (N/A)	5.32	5.29	5.10	5.34	6.14	4.50	4.10	4.33	4.74

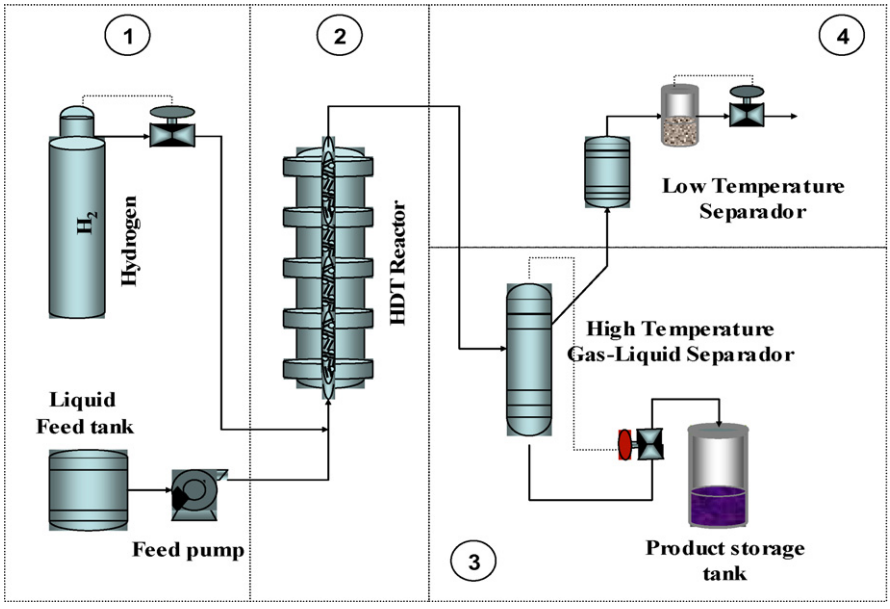

Fig. 2. General scheme of the hydrotreating pilot unit.

liquid hourly space velocity (LHSV) 1–3 h^{-1}, and for gas/oil ratio 4.5–6.25. The normal operating conditions selected for the inhibition tests were: $T = 350\,^{\circ}C$, $P = 10$ MPa, LHSV = 1.1 h^{-1}, gas/oil ratio = 6.24, whereas for severe operating conditions temperatures over 370 °C were considered. The resulting products of hydrotreating were subsequently collected once every 24 h, followed by adjustment of new conditions. At the end, 46 tests, involving different operational conditions, were carried out for kinetic analysis and other 32 tests were done in order to detect inhibition effects (2^5 factorial design).

2.3. Analytical part

After a wide review of analytical techniques to follow the transformation during hydrotreating of real feedstock, a selection was made: ultraviolet–visible spectroscopy (UV–vis) for determination of aromatic families, nuclear magnetic resonance (NMR) for total aromatic content and others, and standard methods (ASTM) for determination of total sulfur, basic nitrogen, and non-basic nitrogen in medium and heavy oil fractions. Other additional analyses such as simulated distillation (SimDis)

Table 2
Selected kinetic models for model discrimination in HDS

Model	Hydrogenolysis	Hydrogenation
1. Girgis and Gates [4]	$r = \frac{kK_{DBT}K_{H_2}C_{DBT}C_{H_2}}{(1+K_{DBT}C_{DBT}+K_{H_2S}C_{H_2S})^2(1+K_{H_2}C_{H_2})}$	$r = \frac{k'K'_{DBT}K'_{H_2}C_{DBT}C_{H_2}}{1+K'_{DBT}C_{DBT}}$
2. Froment et al. [5]	$r_{DBT-CHB} = \frac{k_2K_{DBT,\tau}C_{DBT}C_{H_2}}{(1+K_{DBT,\tau}C_{DBT})^3}$	$r_{DBT-BPH} = \frac{k_1K_{DBT\sigma}K_{H_2,\sigma}C_{DBT}C_{H_2}}{(1+K_{DBT\sigma}C_{DBT}+\sqrt{K_{H_2,\sigma}C_{H_2}}+K_{H_2S,\sigma}(C_{H_2S}/C_{H_2}))^3}$
3. Broderick et al. [6]	$r = \frac{k_2C_{DBT}C_{H_2}}{(1+K_{DBT}C_{DBT}+K_{H_2S}C_{H_2S})^2+(1+K_{H_2}C_{H_2})}$	$r_{DBT-\tau} = \frac{k_2C_{DBT}C_{H_2}}{(1+K_{DBT}C_{DBT})(1+K_{H_2}C_{H_2})}$
4. Avraam and Vasalos [7]	$r_{HDS} = \frac{K^E_{11}C^S_{H_2}C^S_{DBT}}{(1+K^{HDS}_{H_2S}C^S_{H_2S}+K^{HDS}_{A}C^S_{DBT})^2}$	
5. Chen et al. [8]	$r_A = KC_A^{1.12}C_{H_2}^{0.85}$	
6. Van Hasselt et al. [9]	$r_A = \frac{K_rC^2_{DBT}C_{H_2}}{1+KC_{H_2S}}$	
7. Tsamatsoulis and Papayannakos [10]	$r_{HDS} = \frac{k_{HDS}P_{H_2}C_S^{2.3}}{1+K_{H_2S}P_{H_2S}}$	
8. Cotta et al. [11]	$r_A = K_SC^{1.2}_{DBT}P^{1.5}_{H_2}$	
9. Tsamatsoulis and Papayannakos [10]	$r_{HDS} = \frac{k_{HDS}P_{H_2}C_S^{2.16}}{1+K_{H_2S}P_{H_2S}+K_{H_2}P_{H_2}}$	

and saturate-aromatic-resin (SAR) analysis for hydrotreated and non-hydrotreated samples were also selected and used.

3. Kinetic equations

3.1. HDS

For the HDS reactions, sequential design of experiments was used [3]. A set of nine different models of kinetic equations of the Langmuir–Hinshelwood and power type were taken from literature [4–11] (see Table 2). The sequential discrimination procedure, supplemented with a statistical analysis of the data, selected a kinetic model out of nine rival models [6]. The optimal parameter estimation of the final model was made by the minimal volume criteria. A user-friendly computational program was developed based on Matlab 6.5®. Results obtained with this program are in concordance with data reported in literature.

The final kinetic expressions obtained for HDS, HDN and HDA [12] are (all concentrations shown in Eqs. (1)–(4) are catalyst surface concentrations, the subscript "s" has been omitted).

For DBT hydrogenolysis and hydrogenation [6]:

$$r_{\mathrm{DBT}-\sigma} = \frac{k_1 C_{\mathrm{DBT}} C_{\mathrm{H_2}}}{(1 + K_{\mathrm{DBT}} C_{\mathrm{DBT}} + K_{\mathrm{H_2S}} C_{\mathrm{H_2S}})^2 (1 + K_{\mathrm{H_2}} C_{\mathrm{H_2}})} \quad (1)$$

$$r_{\mathrm{DBT}-\tau} = \frac{k_2 C_{\mathrm{DBT}} C_{\mathrm{H_2}}}{(1 + K_{\mathrm{DBT}} C_{\mathrm{DBT}})(1 + K_{\mathrm{H_2}} C_{\mathrm{H_2}})} \quad (2)$$

3.2. HDN

The selected kinetic model is [7]:

$$r_{\mathrm{HDN}} = \frac{k_3 K_{12} C_{\mathrm{N}} C_{\mathrm{H_2}}}{(1 + K_{1,\mathrm{H_2S}} C_{\mathrm{H_2S}} + K_{1,\mathrm{A}} C_{\mathrm{A}})^2} + \frac{(1 - k_3) K_{22} C_{\mathrm{N}} C_{\mathrm{H_2}}}{(1 + K_{2,\mathrm{H_2S}} C_{\mathrm{H_2S}} + K_{2,\mathrm{A}} C_{\mathrm{A}})^2} \quad (3)$$

3.3. HDA

Based on: $A_1 + \alpha H_2 \Leftrightarrow A_2$ [7]:

$$r_{\mathrm{HDA}} = \frac{K_{\mathrm{H_2}} C_{\mathrm{A1}}}{1 + K_{1,\mathrm{H_2S}} C_{\mathrm{H_2S}}} + \frac{K_{\mathrm{D}} C_{\mathrm{A2}}}{1 + K_{1,\mathrm{H_2S}} C_{\mathrm{H_2S}}} \quad (4)$$

where

$$K_{\mathrm{H}} = K_{\mathrm{H},0} P_{\mathrm{H_2}}^{x} \, \mathrm{e}^{-(E/R)((1/T)-(1/T_0))} \quad (5)$$

$$K_{\mathrm{D}} = \frac{K_{\mathrm{H},0}}{K_{\mathrm{P}} P_{\mathrm{H_2}}^{\alpha - x}} \, \mathrm{e}^{-((E-\Delta H)/R)((1/T)-(1/T_0))} \quad (6)$$

4. Reactor model development

4.1. Industrial reactor

The hydrotreating process in the Refinery of Barrancabermeja (ECOPETROL) is carried out through two fixed-bed industrial catalytic reactors with a catalyst load of approximately

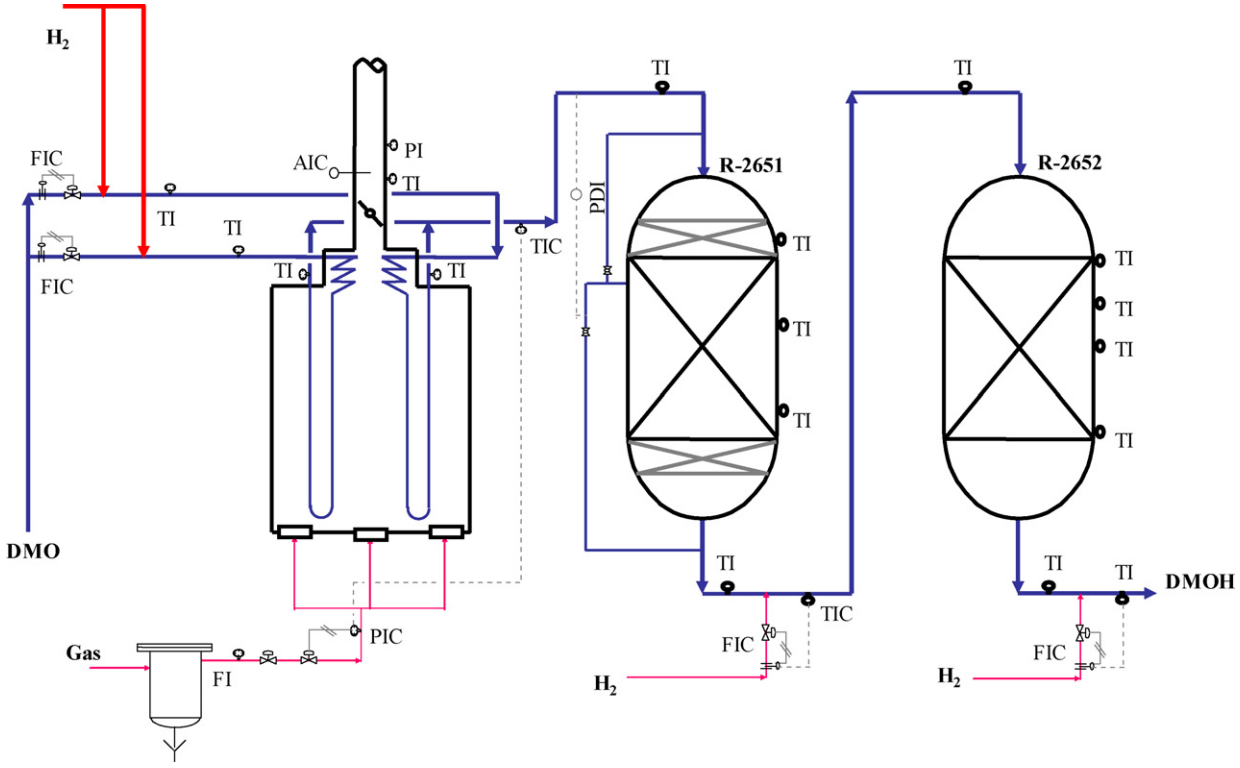

Fig. 3. General scheme of the hydrotreating industrial unit.

40 tonnes each, as shown in Fig. 3. This plant has a processing capacity of 22,000 bbl/day, the main feed is demetalized oil (DMO), deasphalted vacuum bottoms, mixed with gaseous reactants consisting either of pure hydrogen or a mixture of hydrogen, hydrogen sulfide and other light hydrocarbons, then the gas–DMO mixture is heated and led to the first reactor. Typically, these reactors are operated at a pressure of 1500 psi, a maximum temperature of 400 °C, and liquid space hourly velocity (LSHV) of 1.1 h^{-1}.

4.2. Reactor model

Froment et al. [5] reported the challenges related with the modeling of HDT reactors, especially those associated with the hydrodynamics and the complex nature of the feed. To obtain the thermodynamic properties of such a mixture is not a simple task, even if basic data are available or can be estimated. Kinetic aspects are a major element of reactor modeling, but in this case, the transformation of a large number of sulfur and nitrogen compounds made it a formidable problem, and therefore properly assumptions for modeling purposes are needed. In this work, the modeling is focused in three aspects: (1) to obtain a proper reactor model and build the balance equations, (2) to find expressions for physicochemical properties, and (3) to choose the best kinetic expressions for each one of the selected reactions.

4.2.1. TBR model

The use of trickle bed reactors (TBR) for HDT process is well and widely known, because of comparative advantages over other types of reactors. Then, a set of several three-phase reactor models was evaluated [5–18]. Finally, for liquid and gas phases the three-phase model reported by Korsten and Hoffman [16] was selected, and combined with the solid phase, using the model reported by Froment et al. [5]. The model (especially for mass transfer) follows the scheme presented in Fig. 4 (see "Nomenclature").

Taking into account the above-mentioned information the following assumptions and model simplifications were made.

Reactor model is one-dimensional heterogeneous (gas and liquid phases in plug flow). The main reactions are HDS, HDN and mono-, di- and tri-aromatics HDA. The reactions occurred in the liquid phase in contact with the catalyst surface, this means that the reactions occurred between dissolved hydrogen in the liquid phase and the other reactants in the feed. The reactor operates isothermally; it means that catalyst, liquid, and gas are at the same temperature. The liquid volume in the reactor remains constant. External mass transfer is negligible. Uniform pellet properties, catalyst wetting is complete, and there is no catalyst deactivation; and finally, hydrocarbon concentration does not change, and there is no evaporation of liquid.

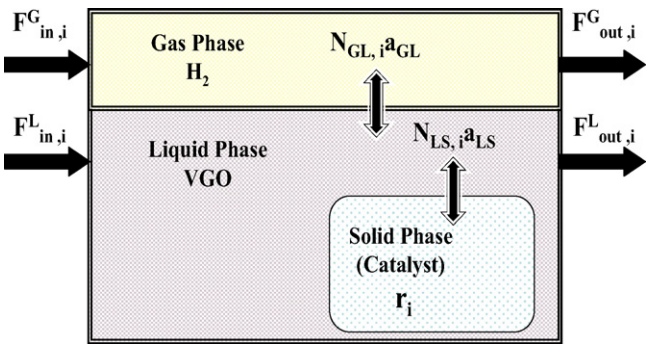

Fig. 4. Mass transfer scheme for the TBR model.

A summary of the main assumptions for modeling and simulation of the hydrotreating reactor for vacuum gas oil, required data, and available tools, is presented in Fig. 5.

4.2.2. Balance equations

The main balance equations of the model [16] are briefly presented.

The mass-balance equation for the gaseous components is:

$$\frac{u_G}{RT}\frac{dp_i^G}{dz} + k_i^L a_L\left(\frac{p_i^G}{H_i} - C_i^L\right) = 0 \tag{7}$$

And for the gaseous compounds in the liquid phase is:

$$u_L\frac{dC_i^L}{dz} - k_i^L a_L\left(\frac{p_i^G}{H_i} - C_i^L\right) + k_i^S a_S(C_i^L - C_i^S) = 0 \tag{8}$$

The mass-balance equation for the organic sulfur compounds and the liquid hydrocarbon is:

$$u_L\frac{dC_i^L}{dz} + k_i^S a_S(C_i^L - C_i^S) = 0 \tag{9}$$

The mass-balance for component i inside spherical catalyst is [5]:

$$\frac{D_{ie}}{r^2}\frac{d}{dr}\left(r^2\frac{dC_{iS}}{dr}\right) = \rho_s\sum_{j=1}^{Nr} S[j,i]r_j(C_{iS},\ldots,T_S) \tag{10}$$

where r is the radial coordinate, with the following boundary conditions:

$$\text{At } r = 0, \qquad \frac{dC_{is}}{dr} = 0 \tag{11}$$

and,

$$\text{at } r = R, \qquad K'(C_i^L - C_i^S) = D_{ei}\frac{dC_i^S}{dr} \tag{12}$$

4.2.3. Physicochemical properties

The proposed model needs correlations for the determination of oil density, Henry coefficient H_i, H_2 solubility, H_2S solubility, gas–liquid mass transfer coefficient, dynamic liquid viscosity, diffusivity D_i, molar volume, liquid–solid mass transfer coefficient, and specific surface area a_S. All these parameters are determined at the process conditions using information reported in literature. These correlations are given by Eqs. (13)–(26) from [16,19,20] (In some cases Engineering Units were reported; where 1 psi = 6894.3 Pa, and 1°R = 1.8 K).

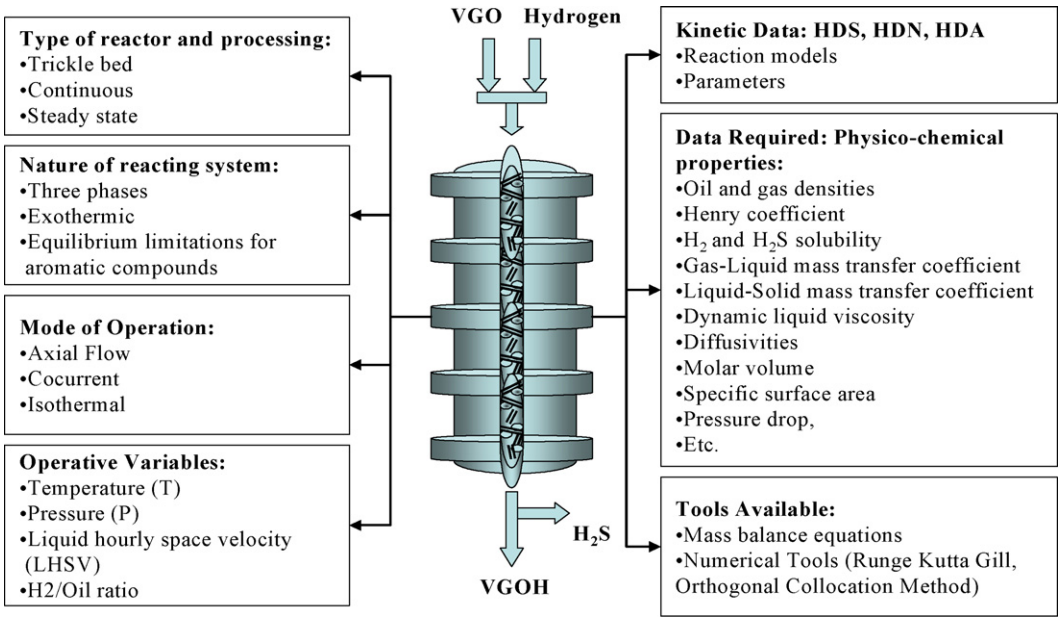

Fig. 5. Assumptions for modeling and simulation of hydrotreating reactor.

Oil density ρ_0 (lb/ft^3) at S.C. correction for high pressure and temperature; P (psia), T (°R):

$$\rho(P,T) = \rho_0 + \Delta\rho_P - \Delta\rho_T \tag{13}$$

$$\Delta\rho_P = [0.167 + (16.181 \times 10^{-0.0425\rho_0})]\left(\frac{P}{1000}\right)^1 - 0.01\,[0.299 + (263 \times 10^{-0.0603\rho_0})]\left(\frac{P}{1000}\right)^2 \tag{14}$$

$$\Delta\rho_T = \left[0.0133 + 152.4(\rho_0 + \Delta\rho_P)^{-2.45}\right](T - 520) - \left[8.1 \times 10^{-6} - 0.0622 \times 10^{-0.764(\rho_0+\Delta\rho_P)}\right] \times (T - 520)^2 \tag{15}$$

Henry coefficient ν_N, molar gas volume at S.C.; ρ_L, liquid density at process conditions:

$$H_i = \frac{\nu_N}{\lambda_i \rho_L} \tag{16}$$

Solubility of hydrogen [(Nl H_2)/(MPa kg oil)], T (°C), ρ_{20} to 20 °C (g/cm^3):

$$\lambda_{H_2} = -0.559729 - 0.42947 \times 10^{-3}T + 3.07539 \times 10^{-3}\left(\frac{T}{\rho_{20}}\right) + 1.94593 \times 10^{-6}T^2 + \frac{0.835793}{\rho_{20}^2} \tag{17}$$

Solubility of H_2S:

$$\lambda_{H_2S} = \exp(3.3670 - 0.008470T) \tag{18}$$

Gas–liquid mass transfer coefficient (s^{-1}) ρ_L previously determined; G_L, liquid superficial mass-flow velocity:

$$\frac{K_i^L a_L}{D_i^L} = 7\left(\frac{G_L}{\mu_L}\right)^{0.4}\left(\frac{\mu_L}{\rho_L D_i^L}\right)^{1/2} \tag{19}$$

Dynamic liquid viscosity (mPa s), T (°R):

$$\mu_L = 3.141 \times 10^{10}(T - 460)^{-3.444}(\log(API))^a \tag{20}$$

$$a = 10.313\log(T - 460) - 36.447 \tag{21}$$

Diffusivity (cm^2/s), T (°K), μ_L (mPa s), v_i, v_L: molar volume of solute and solvent (cm^3/mol):

$$D_i^L = 8.93 \times 10^{-8}\left(\frac{v_L^{0.267}}{v_i^{0.433}}\right)\left(\frac{T}{\mu_L}\right) \tag{22}$$

Molar volume (cm^3/mol), v_c critical specific volume of gaseous compounds:

$$v = 0.285 v_c^{1.048} \tag{23}$$

Critical volume (ft^3/lb), T_{MeABP} (°R) mean average boiling point, $d_{15.6}$ specific gravity at 15.6 °C. v_c^m to v_c carried out by multiplication with molecular weight M:

$$v_c^m = 7.5214 \times 10^{-3}(T_{MeABP}^{0.2895})(d_{15.6}^{-0.7666}) \tag{24}$$

Liquid–solid mass transfer coefficient (s^{-1}):

$$\frac{K_i^S}{D_i^L a_S} = 1.8\left(\frac{G_L}{a_S \mu_L}\right)^{1/2}\left(\frac{\mu_L}{\rho_L D_i^L}\right)^{1/3} \tag{25}$$

Specific surface area d_p equivalent particle diameter, ε void fraction of catalyst bed:

$$a_S = \frac{6}{d_p}(1 - \varepsilon) \tag{26}$$

A specific numerical package was developed for the evaluation of thermodynamic and physicochemical properties of hydrocarbon compounds and mixtures, and for detailed calculation of interfacial mass transfer rates, using information reported in literature [7,16,21]. All variables of the system were considered as dimensionless function of the space variable. Integration in the axial direction (differential equations system) was developed along the reactor length using a fourth order Runge–Kutta–Gill algorithm with variable step size. The intraparticle integration is a boundary value problem which needs suitable treatment; the orthogonal collocation method was successfully used [22,23].

5. Results and discussion

5.1. Operational variables

To improve the sulfur, non-basic, basic nitrogen conversion three procedures can be chosen: increase of temperature, increase of pressure, or decrease of space-velocity. In this work, temperature has the greatest influence on the HDT process compared with the rest of the parameters. High temperatures also favor aromatic saturation. It was observed that the rate of removal of sulfur compounds was faster than for basic-nitrogen (Nb), and non-basic nitrogen (Nnb), under the studied process conditions; however, this behavior is less evident at high temperatures. Similar observations are reported by other researchers [24–27]. The effect of temperature on the conversion of sulfur (S), basic nitrogen (Nb) and non-basic nitrogen (Nnb) during the hydrotreating of the selected vacuum gas oil in the pilot plant is presented in Fig. 6. By increasing the temperature, the hydrodesulfurization (HDS), and the hydrodenitrogenation (HDNb and HDNnb) significantly improved. Fig. 7 shows the transformation of mono-aromatic (MA), di-aromatic (DA), tri-aromatic (TA), and poly-aromatic (PA) compounds. The mono-aromatic content increased, and joint di-, tri- and poly-aromatic content decreased as the temperature was raised. However, the decrease of di-, tri- and poly-aromatic is fast until about 350 °C, and then the decrease is slower. The poly-aromatics are the most reactive compounds. Likewise, the NMR analyses show a decrease in total aromatic hydrogen with an increase in temperature. The

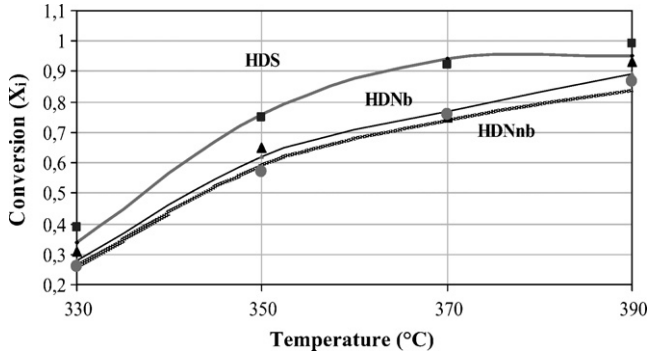

Fig. 6. Simulated (lines) and experimental (points) variations of sulfur (HDS), basic nitrogen (HDNb), and non-basic nitrogen (HDNnb) compounds conversion vs. HDT temperature.

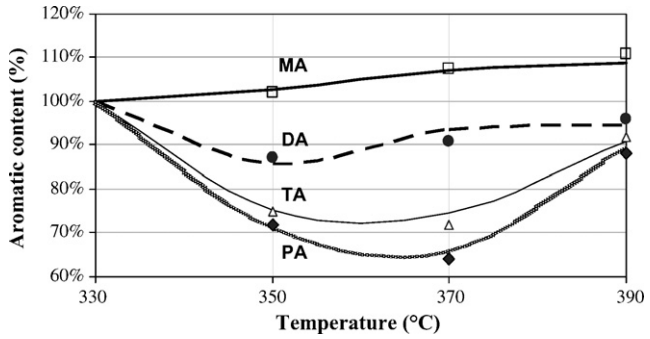

Fig. 7. Simulated (lines) and experimental (points) variations of mono-aromatic (MA) (□), di-aromatic (DA) (●), tri-aromatic (TA) (△), and poly-aromatic (PA) (♦) compounds contents vs. HDT temperature.

established reactivity order (lesser to greater extend in reactivity) was MA/DA/TA/PA at all the studied temperatures; at 370 °C the relationship for reactivity was 1.0/2.0/2.5/3.0, whereas at 390 °C was 1.0/1.5/2.0/2.5, showing that at higher temperatures thermodynamic equilibrium constraints are imposed, mainly for tri- and poly-aromatic reactions, which leads to significant reductions in conversion.

In general, the obtained hydrotreatment reactivity order was: HDS > HDNb > HDNnb > HDA(PA) > HDA(TA) > HDA(DA) > HDA(MA) following the approximately relationship 10.0/9.8/8.5/8.0/6.5/5.0/3.0.

5.2. Trickle bed reactor simulation performance

The results from the developed software showed good agreement between theoretical and experimental data at the exit of the reactor. The concentration profiles for selected compounds along the reactor are showed in Fig. 8 (at a temperature of 350 °C). As the reactor length was increased the mono-aromatics concentration raised, whereas sulfur, nitrogen and total aromatics concentration decreased. On the other hand, the H_2S concentration increased rapidly reaching a maximum value at a medium reactor length and then slowly decreasing. Results from the

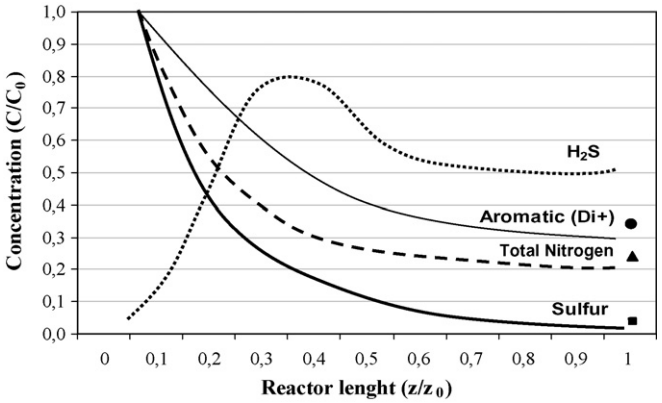

Fig. 8. Simulated (lines) variation of concentrations along the reactor in liquid phase for sulfur, total nitrogen, di+ aromatics and H_2S, and experimental data at the end of the reactor for sulfur (■), total nitrogen (▲) and di+ aromatics (●). $T = 350$ °C, $P = 10$ MPa, LSHV = 1.1 h^{-1}, gas/oil = 6.25. Experimental data for H_2S concentration were not taken and comparative results are not shown.

model were compared with the experimental data from the operation of the pilot plant unit and a notable agreement between the two was obtained. A strong dependence of the rate constant for each selected reaction and of most of physicochemical parameters on the work temperature was observed. A comparison between experimental and calculated mass concentrations of sulfur, nitrogen, and aromatics at the exit of the reactor shows an average absolute error for all predictions of less than 8%.

5.3. Inhibition effects

The proposed methodology of use of a VGO severely hydrotreated (less than 120 ppm sulfur, 20 ppm basic nitrogen, 1% total nitrogen) as a matrix to carry the pure molecules led to important results. The matrix re-hydrotreatment does not produce significant changes in concentrations. Initially, the solubility of some pure molecules in the matrix was not complete, so it was necessary to make a test at high pressures and agitation velocities, in order to obtain emulsions with the chemicals until good solubility was observed. Based on this methodology, inhibitions for the HDS reactions at low and high concentrations of different aromatic molecules such as anthracene, naphthalene, and decahydro-naphthalene were detected. It was found in the present study that increasing the concentration of naphthalene in the feedstock reduces the HDS rates. Likewise, inhibition by basic nitrogen (acridine) and non-basic nitrogen (carbazole) was observed to different extents. In a similar way inhibitions for HDN by sulfur and aromatics molecules were detected. Our results confirm the poisoning effect of carbazol (non-basic) and acridine (basic), even at low concentrations. On the other hand, it was observed that water markedly enhanced the capacity to remove sulfur and nitrogen compounds during HDT of heaviest fractions of VGO's.

6. Conclusions

A sequential design of experiments based on a sequential quadratic programming was used for model discrimination to select a set of significant reactions and estimate their kinetic parameters from pilot plant data. A typical VGO from an industrial refinery was used as a liquid feed. A steady-state heterogeneous model was developed to carry out the simulation of the HDT pilot plant, where HDS, HDN and HDA reactions have been included. The model for the solid phase was solved using orthogonal collocation methods, and for liquid and gas phase using Runge–Kutta methods.

The influence of the main operational variables (T, P, LHSV) in VGO was established, confirming that high temperature, pressure, and low LHSV improve the sulfur and nitrogen conversion. Likewise, the mutual influence of different model molecules (mono-, di-, tri-aromatic, basic nitrogen, non-basic nitrogen, sulfur, water), in a severely hydrotreated vacuum gas oil, was investigated. Light inhibition of HDS reactions by aromatics molecules like naphthalene and phenanthrene, and by basic and non-basic nitrogen compounds like acridine and carbazole, and a promoter effect of water for some HDT reactions in the heavy feed oils were also detected. The good agreement between theoretical and experimental data led to the development of a user-friendly interface software program to facilitate the simulation of the industrial reactor and interpretation of its results. Additionally, in this work it was established that the influence of inhibition effects is significant and therefore further improvement of the kinetic model for simultaneous HDS, HDN and HDA reactions is needed.

Acknowledgements

The authors thank the Colombian Petroleum Institute, ECOPETROL-ICP, for the experimentation and analytical support for this research, and to COLCIENCIAS (Instituto Colombiano para el Desarrollo de la Ciencia y la Tecnología) for a Ph.D. fellowship to F.J. within the frame of the Program for Support of National Doctorates.

References

[1] G. Speight, The Desulfurization of Heavy Oils and Residua, Marcel Dekker, New York, 1981.
[2] K. Altgelt, M. Boduzinski, Composition and Analysis of Heavy Petroleum Fractions, Marcel Dekker, New York, 1994.
[3] G. Froment, K. Bischoff, Chemical Reactor Analysis and Design, John Wiley & Sons, 1990.
[4] M. Girgis, B. Gates, Ind. Eng. Chem. Res. 30 (1991) 2021.
[5] G. Froment, G. Depauw, V. Vanrysselberghe, Ind. Eng. Chem. Res. 33 (1994) 2975.
[6] D.H. Broderick, B.C. Gates, AIChE J. 27 (1981) 663.
[7] D.G. Avraam, I.A. Vasalos, Catal. Today 79 (2003) 275.
[8] J. Chen, Z. Ring, Ind. Eng. Chem. Res. 40 (2001) 3294.
[9] B.W. Van Hasselt, P.J.M. Lebens, H.P.A. Calis, F. Kapteijn, S.T. Sie, J.A. Moulijn, C.M. Van Den Bleek, Chem. Eng. Sci. 54 (1999) 4791.
[10] D. Tsamatsoulis, N. Papayannakos, Chem. Eng. Sci. 53 (1998) 3449.
[11] R.M. Cotta, M.R. Wolf-Maciel, R. Maciel Filho, Comput. Chem. Eng. 24 (2000) 1731.
[12] F. Jiménez, M. Nunez, V. Kafarov, Comp. Aided Chem. Eng. 20 (2005) 619.
[13] Z. Cheng, X. Fanga, R. Zeng, B. Han, L. Huang, W. Yuan, Chem. Eng. Sci. 59 (2004) 5465.
[14] R. Langea, M. Schubert, W. Dietrich, M. Grunewald, Chem. Eng. Sci. 59 (2004) 5355.
[15] R. Chowdhury, E. Pedernera, R. Reimert, AICHE J. 48 (2002) 126.
[16] H. Korsten, U. Hoffman, AICHE J. 42 (1996) 1350.
[17] T. Medjell, R. Myrstad, J. Rosvoll, P. Steiner, Surf. Sci. Catal. 133 (2001) 189.
[18] E. Matos, R. Guirardello, Braz. J. Chem. Eng. 17 (2000) 171.
[19] M.R. Khadilkar, P.L. Mills, M.P. Dudukovic, Chem. Eng. Sci. 54 (1999) 2421.
[20] B. Poling, J. Praustnitz, J. O'Conell, The Properties of Gases and Liquids, Mc Graw Hill, 2001.
[21] M. Rodriguez, J. Ancheyta, Energy Fuels 18 (2004) 789.
[22] B.A. Finlayson, Nonlinear Analysis in Chemical Engineering, Academic Press, 1982.
[23] J. Villadsen, M. Michelsen, Solution of Differential Equation Models by Polynomial Approximation, Prentice Hall Inc., 1978.
[24] S. Bej, A. Dalai, J. Adjaye, Energy Fuels 15 (2001) 377.
[25] J. Ancheyta, M.J. Ángeles, M. Macias, G. Marroquín, R. Morales, Energy Fuels 16 (2002) 189.
[26] D. Ferdous, A. Dalai, J. Adjaye, Energy Fuels 17 (2003) 164.
[27] K. Choi, Y. Korai, I. Mochida, J. Ryu, W. Min, Appl. Catal. B: Environ. 50 (2004) 9.